

The hadronic τ decay of a heavy charged Higgs in models with singlet neutrino in large extra dimensions

Kétévi Adiklè Assamagan

Department of Physics, Brookhaven National Laboratory
Upton, NY 11973 USA

Aldo Deandrea

Institut de Physique Nucléaire, Université de Lyon I
4 rue E. Fermi, F-69622 Villeurbanne Cedex, France

Abstract

We study the LHC sensitivity to the charged Higgs discovery in the channel $H^- \rightarrow \tau_L^- \nu$ in models with a singlet neutrino in large extra dimensions. The observation of such a signal would provide a distinctive evidence for these models since in the standard two Higgs doublet model type II, $H^- \rightarrow \tau_L^- \nu$ is completely suppressed.

PACS: 11.10.Kk, 14.80.Cp, 12.60.Jv

LYCEN-2001-77
November 2001

The hadronic τ decay of a heavy charged Higgs in models with singlet neutrino in large extra dimensions

K  t  vi A. Assamagan*

Department of Physics, Brookhaven National Laboratory, Upton, NY 11973 USA

Aldo Deandrea†

Institut de Physique Nucl  aire, Universit   Lyon I,
4 rue E. Fermi, F-69622 Villeurbanne Cedex, France
(Dated: November, 2001)

We study the LHC sensitivity to the charged Higgs discovery in the channel $H^- \rightarrow \tau_L^- \nu$ in models with a singlet neutrino in large extra dimensions. The observation of such a signal would provide a distinctive evidence for these models since in the standard two Higgs doublet model type II, $H^- \rightarrow \tau_L^- \nu$ is completely suppressed.

PACS numbers: 1.10.Kk, 14.80.Cp, 12.60.Jv

I. INTRODUCTION

The possibility that our world has more than four space-time dimensions has been considered long time ago [1]. More recently phenomenological studies based on simplified models have brought new insight on how extra dimensions may show up in present and future experimental setups. Localization of Standard Model (SM) degrees of freedom on a (3+1)-dimensional wall or 3-brane explains why low energy physics is effectively four dimensional [2]. In models where extra dimensions open up at the TeV scale, small neutrino masses can be generated without implementing the seesaw mechanism [3]. These models postulate the existence of δ additional spatial dimensions of size R where gravity and perhaps other fields freely propagate while the SM degrees of freedom are confined to (3+1)-dimensional wall (4D) of the higher dimensional space. The idea that our world could be a topological defect of a higher-dimensional theory [4] finds a natural environment in string theory [5].

The true scale of gravity, or fundamental Planck scale M_* , of the $(4 + \delta)$ D space time is related to the reduced 4D Planck scale M_{Pl} , as:

$$M_{Pl}^2 = R^\delta M_*^{\delta+2}, \quad (1)$$

where $M_{Pl} = 2.4 \times 10^{18}$ GeV is related to the usual Planck mass 1.2×10^{19} GeV = $\sqrt{8\pi} M_{Pl}$. Since no experimental deviations from Newtonian gravity are observed at distances above 0.2 mm [6], the extra dimensions must be at the sub-millimeter level with M_* as low as few TeV and $\delta \geq 2$.

The right handed neutrino can be interpreted as a singlet with no quantum numbers to constrain it to the SM brane and thus, it can propagate into the extra dimensions just like gravity [7]. Such singlet states in the bulk

couple to the SM states on the brane as right handed neutrinos with small couplings – the Yukawa couplings of the bulk fields are suppressed by the volume of the extra dimensions. The interactions between the bulk neutrino and the wall fields generate Dirac mass terms between the wall fields and all the Kaluza-Klein modes of the bulk neutrino. As long as this mass is less than $1/R$, the Kaluza-Klein modes are unaffected while for the zero mode, the interaction generates a Dirac neutrino mass suppressed by the size of the extra dimensions:

$$m_D = \frac{\lambda}{\sqrt{2}} \frac{M_*}{M_{Pl}} v \quad (2)$$

where λ is a dimensionless constant and v the Higgs vacuum expectation value (VEV), $v \simeq 246$ GeV. The mixing between the lightest neutrino with mass m_D and the heavier neutrinos introduces a correction N to the Dirac mass such that the physical neutrino mass m_ν is [3]:

$$m_\nu = \frac{m_D}{N}, \quad (3)$$

where

$$N \simeq 1 + \sum_{\vec{n}}^{| \vec{n} | < M_* R} \left(\frac{m_D R}{\vec{n}} \right)^2, \quad (4)$$

\vec{n} is a vector with δ integer components counting the number of states and the summation is taken over the Kaluza-Klein states up the fundamental scale M_* . The sum over the different Kaluza-Klein states can be approximately replaced by a continuous integration. The following formula can be used:

$$\sum_{\vec{n}}^{| \vec{n} | < M_* R} f \left(\frac{\vec{n}^2}{R^2} \right) \longrightarrow S_\delta R^\delta \int_0^{M_*} dx x^{\delta-1} f(x^2), \quad (5)$$

where f is a function of \vec{n}^2/R^2 and $S_\delta = 2\pi^{\delta/2}/\Gamma(\delta/2)$ is the surface of a unit radius sphere in δ dimensions. After

*Electronic address: ketevi@bnl.gov

†Electronic address: deandrea@ipnl.in2p3.fr

summing over Kaluza-Klein states up to the cut-off M_* , assuming $\delta \neq 2$:

$$N \simeq 1 + \left(\frac{m_D}{M_*} \right)^2 \left(\frac{M_{Pl}}{M_*} \right)^2 \frac{2\pi^{\delta/2}}{\Gamma(\delta/2)} \frac{1}{\delta - 2}. \quad (6)$$

As shown in Table I, small neutrino masses, m_ν , can be obtained consistent with atmospheric neutrino oscillations [8].

The framework of singlet neutrino in large extra dimensions must satisfy some phenomenological constraints: for $\delta = 2$, the mixing between the lightest state and the higher Kaluza-Klein excitations can be of $O(1)$ and therefore problematic since in such a case $m_D < 1/R$ is no longer valid. In addition, due to such a large mixing, this scenario might run into problem with nucleosynthesis [2, 3, 7] (we consider $\delta > 2$ in this analysis). Finally, too much energy could be dissipated into the bulk neutrino modes, leading to an unacceptable expansion rate of the universe if $m_D^2 \geq 10^{-3}$ (eV)² and $1/R \leq 10$ keV [2, 11] (we confine this analysis to the parameter space where this constraint is satisfied).

The spectrum of many extensions of the SM includes a charged Higgs state. We consider as a prototype of these models the 2-Higgs Doublet Model of type II (2HDM-II), where the Higgs doublet with hypercharge $-1/2$ couples only to right-handed up-type quarks and neutrinos whereas the $+1/2$ doublet couples only to right-handed charged leptons and down-type quarks; an example is the Minimal Supersymmetric Standard Model (MSSM). In the following we will continue to use the VEV $v \simeq 246$ GeV as in formula (2). Its meaning in terms of v_1 (VEV of the $+1/2$ doublet) and v_2 (VEV of the $-1/2$ doublet) is the usual one:

$$\frac{v}{\sqrt{2}} = \sqrt{v_1^2 + v_2^2} \quad \tan \beta = \frac{v_2}{v_1} \quad (7)$$

H^- decays to the right handed τ^- through the τ Yukawa coupling:

$$H^- \rightarrow \tau_R^- \bar{\nu}. \quad (8)$$

The H^- decay to left handed τ^- is completely suppressed in MSSM. However, in the scenario of singlet neutrino in large extra dimensions, H^- can decay to both right handed and left handed τ^- depending on the parameters M_* , m_D , δ , m_{H^\pm} and $\tan \beta$:

$$H^- \rightarrow \tau_R^- \bar{\nu} + \tau_L^- \psi, \quad (9)$$

where ψ is a bulk neutrino and ν is dominantly a light neutrino with a small admixture of the Kaluza-Klein modes of the order $mR/|n|$. The measurement of the polarization asymmetry,

$$A = \frac{\Gamma(H^- \rightarrow \tau_L^- \psi) - \Gamma(H^- \rightarrow \tau_R^- \bar{\nu})}{\Gamma(H^- \rightarrow \tau_L^- \psi) + \Gamma(H^- \rightarrow \tau_R^- \bar{\nu})}, \quad (10)$$

can be used to distinguish between the ordinary 2HDM-II and the scenario of singlet neutrino in large extra dimensions – depending on the parameters – since in the

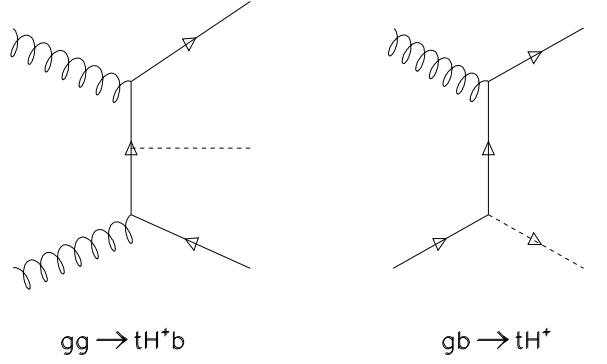


FIG. 1: The charged production at the LHC through the $2 \rightarrow 3$ process, $gg \rightarrow tbH^\pm$ and the $2 \rightarrow 2$ process, $gb \rightarrow tH^\pm$. The inclusive cross section is the sum of both contributions after the subtraction of the common terms. In the framework of large extra dimensions with singlet neutrino in the bulk, there are no additional Higgs bosons. Thus, the charged Higgs productions are the same as in the 2HDM-II.

2HDM-II, the polarization asymmetry would be -1.0 . In this framework of large extra dimensions, the polarization asymmetry could also be -1.0 if the left handed τ component of the decay (9) is completely suppressed. In such a case, the decay of H^- would be similar to the 2HDM-II case but possibly with a different phase space since the neutrino contains some admixture of the Kaluza-Klein modes.

The singlet neutrino may not necessarily propagate into the δ -extra dimensional space. It is possible to postulate that the singlet neutrino propagate into a subset δ_ν ($\delta_\nu \leq \delta$) of the δ additional spatial dimensions, in which case the formalism for the generation of small Dirac neutrino masses is merely a generalization of the case $\delta_\nu = \delta$ discussed above [2].

The charged Higgs decay to right handed τ , $H^- \rightarrow \tau_R^- \bar{\nu}$ have been extensively studied for the LHC [9, 10]. In this paper, we discuss the possibility to observe $H^- \rightarrow \tau_L^- \psi$ at the LHC above the top-quark mass. Table I shows the parameters selected for the current analysis. The cases where the asymmetry is $+1$ are discussed in details. We assume a heavy SUSY spectrum with maximal mixing. The present analysis is conducted in the framework of PYTHIA6.1 [12] and ATLFast [13], and the Higgs masses and couplings are calculated to 1-loop with FeynHiggsFast [14].

II. H^\pm PRODUCTION AND DECAYS

In this framework, no additional Higgs bosons are needed. As a result, the charged Higgs productions are the same as in the 2HDM-II, shown in Fig. 1. We consider the $2 \rightarrow 2$ production process where the charged Higgs is produced with a top-quark, $gb \rightarrow tH^\pm$. Further, we re-

TABLE I: The parameters used in the current analysis of the signal with the corresponding polarization asymmetry. In general, H^- would decay to τ_L^- and τ_R^- , $H^- \rightarrow \tau_R^- \bar{\nu} + \tau_L^- \psi$, depending on the asymmetry. For the decay $H^- \rightarrow \tau_R^- \bar{\nu}$ (as in MSSM), the asymmetry is -1 and this case is already studied for the LHC [9, 10]. The signal to be studied is $H^- \rightarrow \tau_L^- \psi$.

	M_* (TeV)	δ_ν	δ	m_D (eV)	m_{H^\pm} (GeV)	$\tan \beta$	Asymmetry	m_ν (eV)
Signal-1	2	4	4	3.0	219.9	30	~ 1	$0.5 \cdot 10^{-3}$
Signal-2	20	3	3	145.0	365.4	45	~ 1	0.05
Signal-3	1	5	6	5.0	506.2	4	~ 1	0.05
Signal-4	100	6	6	0.005	250.2	35	~ -1	0.005
Signal-5	10	4	5	0.1	350.0	20	~ -1	0.04
Signal-6	50	5	5	0.04	450.0	25	~ -1	0.04

quire the hadronic decay of the top-quark, $t \rightarrow Wb \rightarrow jjb$ and the charged Higgs decay to τ -leptons. The studies reported in [9, 10] were carried out in MSSM where, as previously stated, the H^- would decay to right handed τ -leptons: $H^- \rightarrow \tau_R^- \bar{\nu}$. In the scenario of large extra dimensions, the τ decay of charged Higgs would contain both left and right handed τ -leptons depending on the asymmetry: $H^- \rightarrow \tau_R^- \bar{\nu} + \tau_L^- \psi$. The right handed component, $H^- \rightarrow \tau_R^- \bar{\nu}$, is similar to the MSSM case up to some phase space factors, in which case the details of the analysis would not differ from [9, 10]. The objective of the current work is to study the LHC sensitivity to the left handed component, $H^- \rightarrow \tau_L^- \psi$. The detection of such a signal could provide a distinctive evidence for models such as large extra dimensions with singlet neutrino in the bulk. However, further measurements – of the rate and the polarization asymmetry – would be necessary to identify the actual scenario that is realized.

The major backgrounds are the single top production $gb \rightarrow Wt$, and $t\bar{t}$ production with one $W^+ \rightarrow jj$ and the other $W^- \rightarrow \tau_L^- \bar{\nu}$. Depending on the polarization asymmetry (see Equation 10), $H^- \rightarrow \tau_R^- \bar{\nu}$ will contribute as an additional background. In Table II, we list the rates for the signal and for the backgrounds. For the phenomenological analysis, it is convenient to express the partial widths in terms of inclusive formulas, where the contributions of the Kaluza-Klein modes are summed up to the kinematical limit $m_\psi \leq m_H$ as the τ mass can be neglected. The partial width of the Higgs decays to $\tau\nu$ depends of the parameters M_* , m_D , δ , m_{H^\pm} and $\tan \beta$ [16]:

$$\Gamma(H^- \rightarrow \tau_L^- \psi) \simeq \frac{m_{H^\pm}}{8\pi} \left(\frac{m_D}{v} \right)^2 \frac{\chi_\delta}{\tan^2 \beta} (m_{H^\pm} R)^\delta, \quad (11)$$

where $(m_{H^\pm} R)^\delta$ is the number of Kaluza-Klein modes lighter than the charged Higgs mass and χ_δ includes the phase space integral:

$$\chi_\delta \simeq \frac{2\pi^{\delta/2}}{\Gamma(\delta/2)} \left(\frac{1}{\delta} - \frac{2}{\delta+2} + \frac{1}{\delta+4} \right). \quad (12)$$

Using the relation (1),

$$(m_{H^\pm} R)^\delta = \left(\frac{m_{H^\pm}}{M_*} \right)^\delta \times \left(\frac{M_{Pl}}{M_*} \right)^2. \quad (13)$$

For the H^- decay to the right handed τ , we have [16]

$$\Gamma(H^- \rightarrow \tau_R^- \bar{\nu}) \simeq \left[\Gamma(H^- \rightarrow \tau_R^- \bar{\nu})_{\text{MSSM}} \right] \frac{[1 + f(m_D, M_*, \delta)]}{N^2} \quad (14)$$

and the normalization factor N is given by Equation (6) and the function $f(m_D, M_*, \delta)$ is (for $\delta \neq 2$):

$$f(m_D, M_*, \delta) = \frac{m_D^2 m_H^{\delta-2}}{M_*^\delta} \left(\frac{M_{Pl}}{M_*} \right)^2 \frac{2\pi^{\delta/2}}{\Gamma(\delta/2)} \times \left(\frac{1}{\delta-2} - \frac{2}{\delta} + \frac{1}{\delta+2} \right). \quad (15)$$

One can generalize these formulas for a singlet neutrino in a smaller number of extra dimensions $\delta_\nu < \delta$ than the extra dimensions available to gravity [3]. Assuming that all the extra dimensions are of the same size R , one has to replace in formulas (6) and (11–15):

$$\delta \rightarrow \delta_\nu \quad \left(\frac{M_{Pl}}{M_*} \right)^2 \rightarrow \left(\frac{M_{Pl}}{M_*} \right)^{2(\delta_\nu/\delta)} \quad (16)$$

The more general case of a non-symmetric internal δ -dimensional manifold is given in [3].

Depending on the parameters M_* , m_D , δ , m_{H^\pm} and $\tan \beta$, the $\tau\nu$ decay of the charged Higgs can be enhanced or suppressed compared to the MSSM case. In Fig. 2 and Fig. 3, we show few cases of how the other decays of the charged Higgs are affected in this framework; for the chosen values of M_* and δ , the decay branchings are similar to MSSM for small values of m_D while at larger m_D , the $\tau\nu$ decay mode becomes strongly enhanced, especially at low $\tan \beta$. In Fig. 4, we show the polarization asymmetry as a function of the charged Higgs mass and for different values of m_D and $\tan \beta$: for small m_D , right handed τ 's are produced, except at low $\tan \beta$ while the asymmetry increases with m_D (see Equation 11). For very large values of M_* and small m_D , we recover the MSSM case as shown in Fig. 5 irrespective of the values of δ considered.

In general, $H^- \rightarrow \tau_L^- \psi + \tau_R^- \bar{\nu}$ with the asymmetry between -1 and 1 . However, the study of $H^- \rightarrow \tau_R^- \bar{\nu}$ has been carried out in detail and reported elsewhere [9, 10]. Therefore, in the current study, we consider the parameters shown in Table I and Table II for which the asymmetry is one, i.e., $H^- \rightarrow \tau_L^- \psi$.

TABLE II: The expected rates ($\sigma \times \text{BR}$), for the signal $gb \rightarrow tH^\pm$ with $H^\pm \rightarrow \tau_R^- \bar{\nu} + \tau_L^- \psi$ and $t \rightarrow jjb$, and for the backgrounds: Wt and $t\bar{t}$ with $W^- \rightarrow \tau_L^- \bar{\nu}$ and $W^+ \rightarrow jj$. We assume an inclusive $t\bar{t}$ production cross section of 590 pb. Other cross sections are taken from PYTHIA 6.1 with CTEQ5L parton distribution function. See Table I for the parameters used for Signal-1, Signal-2 and Signal-3. In the last columns, we compare the $H^\pm \rightarrow \tau\nu$ branching ratios in this model to the corresponding MSSM branching ratios from HDECAY [15].

Process	$\sigma \times \text{BR}$ (pb)	$\text{BR}(H^\pm \rightarrow \tau\nu + \tau\psi)$	MSSM: $\text{BR}(H^\pm \rightarrow \tau\nu)$
Signal-1	1.56	0.73	0.37
Signal-2	0.15	1.0	0.15
Signal-3	0.04	1.0	0.01
$t\bar{t}$	84.11		
$gb \rightarrow Wt$ ($p_T > 30$ GeV)	47.56		

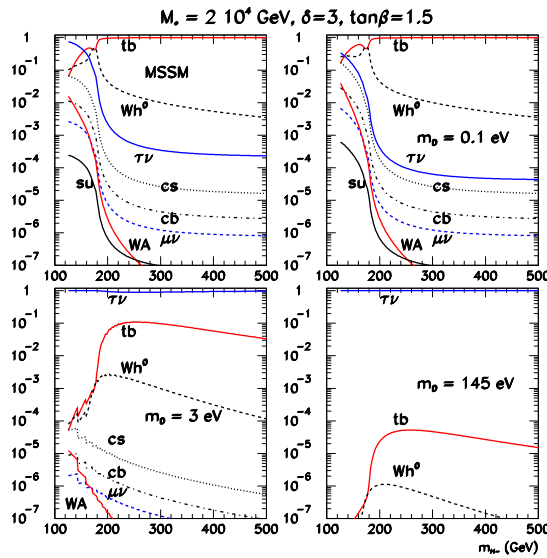


FIG. 2: Charged Higgs decays in models with a singlet neutrino in large extra dimensions for $M_* = 2 \times 10^4$ GeV, $\delta = 3$ and $\tan\beta = 1.5$. For small values of m_D , we see similar decay branchings as in MSSM. As m_D gets larger, $H^\pm \rightarrow \tau\nu$ becomes dominant below and above the top-quark mass.

III. ANALYSIS

The polarization of the τ -lepton is included in this analysis through TAUOLA [17]. We consider the hadronic one-prong decays of the τ -lepton since these are believed to carry a better imprint of the τ -polarization [18]:

$$\tau^- \rightarrow \pi^- \nu \quad (11.1\%) \quad (17)$$

$$\tau^- \rightarrow \rho^- (\rightarrow \pi^- \pi^0) \nu \quad (25.2\%) \quad (18)$$

$$\tau^- \rightarrow a_1^- (\rightarrow \pi^- \pi^0 \pi^0) \nu \quad (9.0\%) \quad (19)$$

In Fig. 6, we show the effects of the τ polarization in the signal and the backgrounds in the case of one-prong $\tau^- \rightarrow \pi^- \nu$. For the signal in MSSM, right handed τ_R^- 's

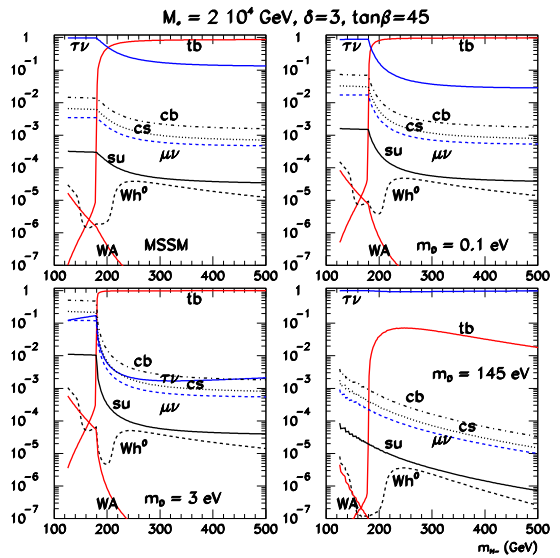


FIG. 3: Charged Higgs decays in models with a singlet neutrino in large extra dimensions for $M_* = 2 \times 10^4$ GeV, $\delta = 3$ and $\tan\beta = 45$. The dependence in m_D is similar to the situation of Fig. 2.

come from the charged Higgs decay, $H^- \rightarrow \tau_R^- \bar{\nu}$, while in the backgrounds, left handed τ_L^- 's come from the decay of the $W^- (\rightarrow \tau_L^- \bar{\nu})$. Since the charged Higgs is a scalar and the W^- a vector, the polarization of the τ results in a stronger τ -jet in the MSSM signal than in the backgrounds for $\tau^- \rightarrow \pi^- \nu$ and longitudinal ρ and a_1 [10, 18]. The studies reported in [9, 10] take advantage of this polarization effect in suppressing the backgrounds further by demanding that the charged track carries a significant part of the τ -jet energy:

$$p_\pi/E^{\tau\text{-jet}} > 80\%. \quad (20)$$

For the signal in MSSM, this requirement would retain only the π and half of the longitudinal ρ and a_1 contributions while eliminating the transverse components along with the other half of the longitudinal contribu-

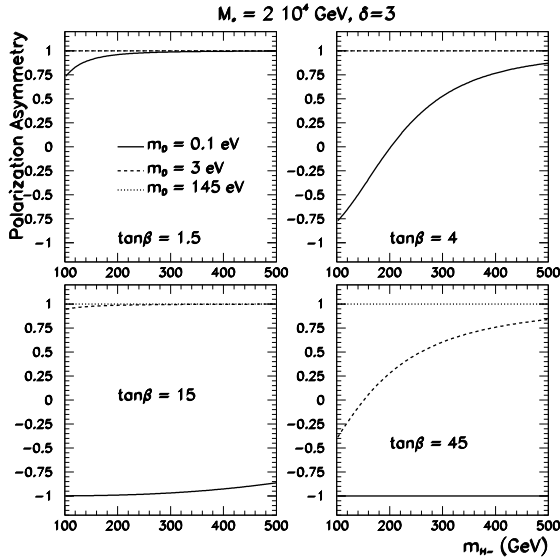


FIG. 4: The polarization asymmetry as a function of m_{H^\pm} , for various values of $\tan\beta$ and m_D . For small values of m_D , the decay τ^- are right handed (except for small $\tan\beta$ values) while left handed τ^- 's are produced as m_D gets larger.

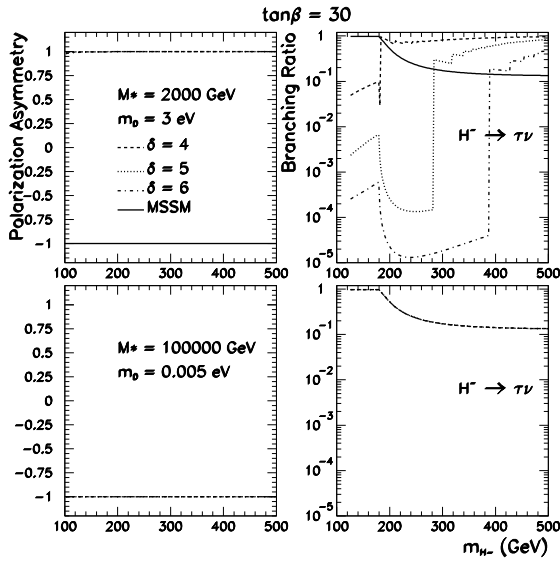


FIG. 5: The polarization asymmetry and the $H^\pm \rightarrow \tau\nu$ branching ratio for two values of (M_*, m_D) and $\delta = 4, 5$ and 6. For very large M_* and small m_D , we recover the MSSM case, i.e., an asymmetry of -1 (right handed τ^-) and MSSM branching ratios (bottom plots).

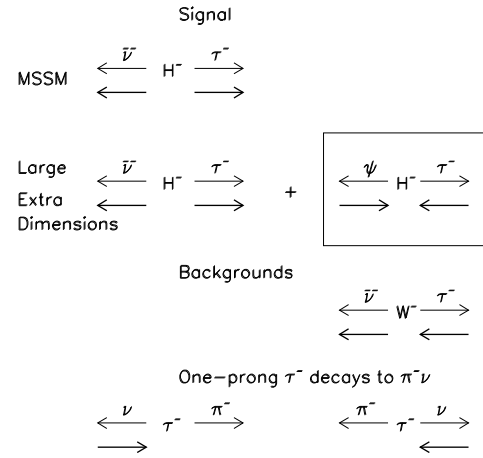


FIG. 6: Polarization of the decay τ from H^\pm in MSSM and in models with a singlet neutrino in large extra dimensions. In the latter case, both left and right handed τ 's can be produced with some polarization asymmetry. In the backgrounds, the τ comes from the decay of the W^\pm . The signal to be studied is in the box — the polarization of the decay τ in this signal is the same as in the background. Thus, τ polarization effects would not help in suppressing the backgrounds but they may help distinguish between the 2HDM and other models.

tions as can be seen from Fig. 7. However, this requirement would suppress much of the backgrounds, shown in Fig. 8. In the framework of large extra dimensions, we are interested in $H^- \rightarrow \tau_L^- \psi$ where, as shown in Fig. 6, the polarization of the τ -lepton would be identical to the background case but opposite to the MSSM case. Therefore, the requirement (20) would not help in suppressing the backgrounds, as can be seen from Fig. 8 and Fig. 9. Nevertheless, there are still some differences in the kinematics which can help reduce the background level, and we discuss the details of the analysis as follow:

- (a) Search for one-prong hadronic τ decays with one τ -jet, $p_T^\tau > 30$ GeV and $|\eta^\tau| \leq 2.5$, at least three non τ jets with $p_T^{\text{jet}} > 30$ GeV. One of these jets must be a b-tagged jet with $|\eta^b| < 2.5$. Further, we apply a b-jet veto by requiring only a single b-jet with $|\eta| \leq 2.0$ and $p_T > 50$ GeV. We assume a τ -jet identification efficiency of 30% and a b-tagging efficiency of 50%, for an integrated luminosity of 100 fb^{-1} . We further assume a multi-jet trigger with a high level τ trigger.
- (b) The W from the associated top-quark is reconstructed and the candidates satisfying $|m_{jj} - m_W| \leq 25$ GeV are retained (and their four-momenta are renormalized to the W mass) for the

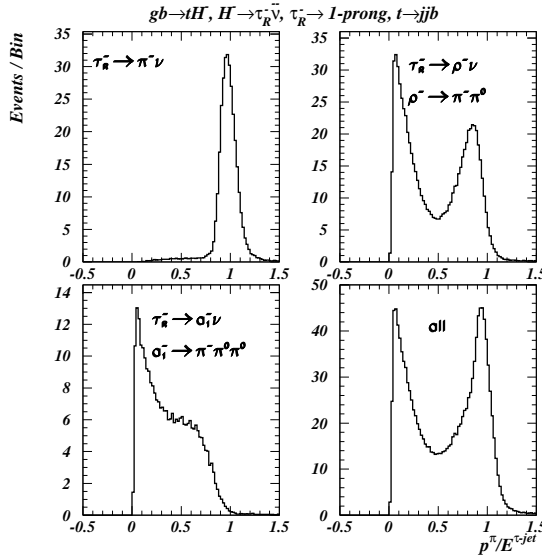


FIG. 7: The one prong decays of the τ -lepton from the signal in MSSM: $H^- \rightarrow \tau_R^- \bar{\nu}$. We plot the ratio of the momentum carried by the charged track to the τ -jet energy. This ratio peaks near 1 for $\tau \rightarrow \pi\nu$ and near 0 and 1 for longitudinal ρ and a_1 . For transverse ρ and a_1 , this ratio peaks in the middle.

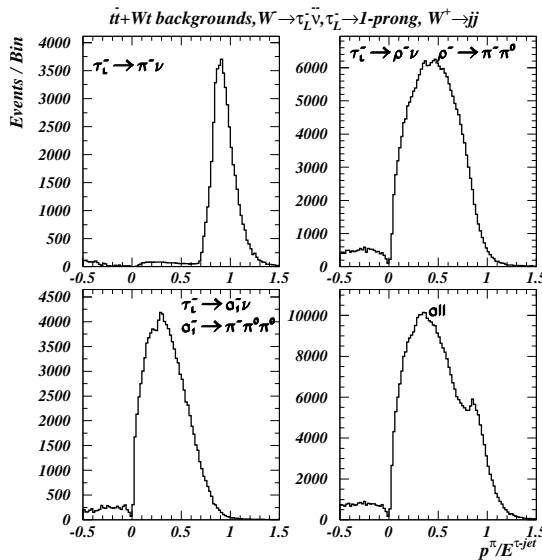


FIG. 8: The one prong decays of the τ -lepton from the $t\bar{t}$ and Wt backgrounds: $W^- \rightarrow \tau_L^- \bar{\nu}$. Here the situation should be reversed and it is for the ρ and a_1 . For $\tau \rightarrow \pi\nu$, the ratio should peak near 0; the peak near 1 comes from the τ -jet labeling criteria in ATLFEST: a jet is labeled a τ -jet by requiring the hadronic decay products to carry a significant fraction (> 0.9) of the τ -jet energy within a jet cone ($\Delta R < 0.3$). For $\tau \rightarrow \pi\nu$, these criteria would select charged pions with this ratio near 1.

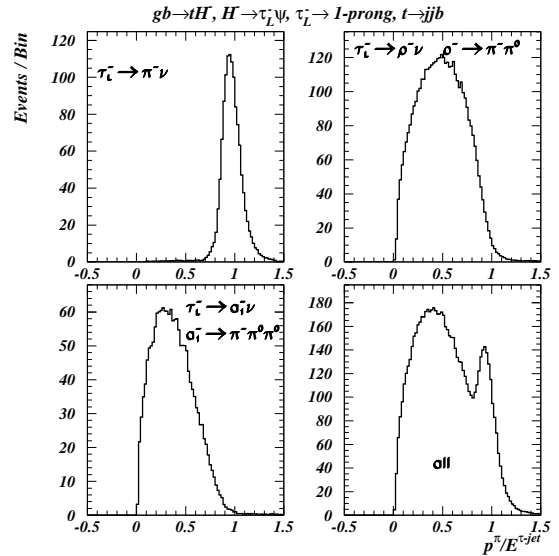


FIG. 9: The one prong decays of the τ -lepton from the signal in models with a singlet neutrino in large extra dimensions with a polarization asymmetry of 1: $H^- \rightarrow \tau_L^- \psi$. (The τ^- from H^- decays are 100% left handed). The situation is thus similar to the backgrounds but opposite to signal in MSSM.

reconstruction of the top-quark: this is done by minimizing the variable $\chi^2 = (m_{jjb} - m_t)^2$. We take $m_W = 80.14$ GeV and $m_t = 175$ GeV. Subsequently, the events satisfying $|m_{jjb} - m_t| < 25$ GeV are retained for further analysis.

(c) We raise the cut on p_T^τ , *i.e.*, $p_T^\tau > 100$ GeV. To satisfy this p_T^τ cut, the τ jet from the backgrounds needs a large p_T boost from the W boson. This will result in a smaller opening angle, $\Delta\phi$, between the decay products $\tau\nu$. $\Delta\phi$ is the azimuthal opening angle between the τ jet and the missing transverse momentum. In the signal $H^\pm \rightarrow \tau\nu$, the τ jet will require little or no boost at all to satisfy this high p_T^τ cut. This explains the backward peak in the $\Delta\phi$ distribution for the signal as shown in Figures 10 and 11 – this backward peak in $\Delta\phi$ is more pronounced as the Higgs mass increases. Similarly, the missing transverse momentum \not{p}_T and the transverse momentum of the τ -jet are increasingly harder for the signal as the Higgs mass increases as seen in Figures 10 and 11. Because of the neutrino in the final state,

$$m_T = \sqrt{2p_T^\tau \not{p}_T [1 - \cos(\Delta\phi)]} \quad (21)$$

can be reconstructed. In the backgrounds, the transverse mass has an upper bound at the W^- mass ($W^- \rightarrow \tau^- \nu$) while in the signal, it is constrained by the charged Higgs mass ($H^- \rightarrow \tau^- \nu$). However, due to the experimental resolution of

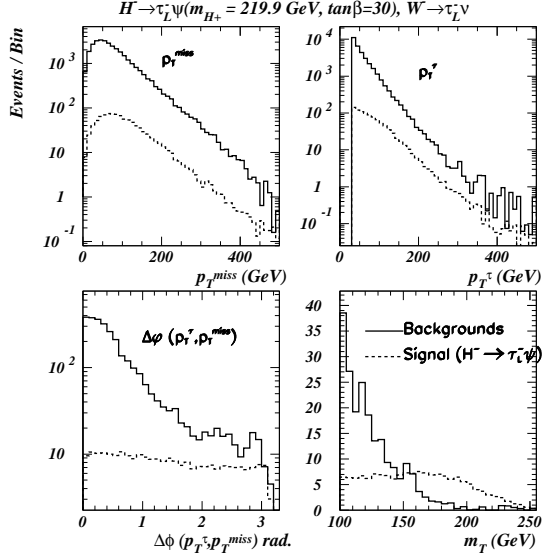


FIG. 10: The reconstructions of p_T^{miss} , the τ -jet transverse momentum, $p_T^{\tau-jet}$ (top plots), the azimuthal opening angle between p_T^{miss} and $p_T^{\tau-jet}$ and the transverse charged Higgs mass (bottom plots) for the signal, $H^- \rightarrow \tau_L^- \psi$ ($m_A = 200$ GeV, $\tan \beta = 30$) and the backgrounds $W^- \rightarrow \tau_L^- \bar{\nu}$. In the signal, the transverse mass is bound from above by the charged Higgs mass while in the backgrounds, the transverse mass is constrained by the W mass. However, due to the E_T^{miss} resolution, we see a “leak” into the signal region.

E_T^{miss} , the m_T distribution for the backgrounds shows a “leak” into the signal region as can be seen in Figures 10 and 11.

- (d) To optimize the signal-to-background ratios and the signal significances, we apply a cut on the missing transverse momentum: $\not{p}_T > 100$ GeV.
- (e) A final cut of $\Delta\phi > 1.0$ rad is applied and the results are shown in Fig. 12 and used for the calculation of the signal-to-background ratios and the signal significances shown in Table III. The reconstruction of the transverse mass, shown in Fig. 12 is not enough to distinguish between the MSSM and the singlet neutrino in large extra dimensions. The differences in these two scenarios are best seen in the distribution of $p^\pi/E^{\tau-jet}$, the fraction of the energy carried by the charged track which is shown in Figures 13 and 14. In MSSM, this distribution peaks near 0 and 1 while in $H^- \rightarrow \tau_L^- \psi$ from large extra dimensions and in the backgrounds, this distribution peaks in the center. The backgrounds are relatively very small, and as concluded in [9] and [10], the discovery reach is limited by the signal size itself. Therefore the observation of a signal in the transverse mass distribution and in the distribution of the fraction of the energy carried by

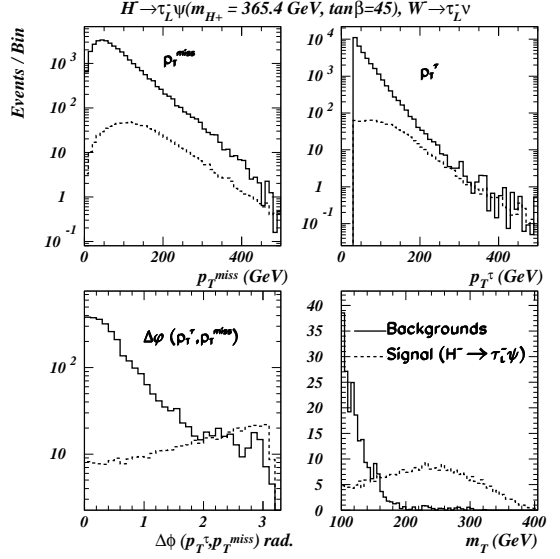


FIG. 11: The reconstructions of p_T^{miss} , the τ -jet transverse momentum, $p_T^{\tau-jet}$ (top plots), the azimuthal opening angle between p_T^{miss} and $p_T^{\tau-jet}$ and the transverse charged Higgs mass (bottom plots) for the signal, $H^- \rightarrow \tau_L^- \psi$, ($m_A = 350$ GeV, $\tan \beta = 45$) and the backgrounds $W^- \rightarrow \tau_L^- \bar{\nu}$. p_T^{miss} and $p_T^{\tau-jet}$ are harder in the signal particularly at higher Higgs mass, and the opening angle $\Delta\phi(p_T^{\tau-jet}, p_T^{miss})$ peaks forward in the backgrounds and backward in the signal.

the charged track should help determine whether the scenario is MSSM or not.

The main effects responsible for the suppression of the backgrounds are: the azimuthal opening angle — between the τ -jet and the missing transverse momentum — which peaks forward in the backgrounds ($W^\pm \rightarrow \tau\nu$) and backward in the signal ($H^\pm \rightarrow \tau\psi$); and the difference in the kinematic bounds on the transverse mass — this bound is at the W-mass in the backgrounds whereas in the signal, the bound is at the charged Higgs mass. The overall efficiencies of the kinematic cuts (c), (d) and (e) might change as a result of the event by event difference in the neutrino mass m_ψ leading to an overall change in the signal-to-background ratios and signal significances of Table III but the results of Figures 12, 13 and 14 would not be affected because these results rely on the differences in the τ -polarization and in the kinematic bounds on the transverse mass, irrespective of the neutrino mass m_ψ . In Table III, we present results for 3 different values of the number of extra dimensions. With different mass distributions of m_ψ depending on the number of extra dimensions, the overall efficiencies for the cuts (c), (d) and (e) might change differently for each of the cases presented in Table III.

TABLE III: The expected signal-to-background ratios and significances calculated after cut (e) for an integrated luminosity of 100 fb^{-1} (one experiment). See Table I for the parameters used for Signal-1, Signal-2 and Signal-3. In all the cases considered, the signal can be observed at the LHC with significances in excess of 5σ at high luminosity.

	Signal-1	Signal-2	Signal-3
Signal events	41	215	16
$t\bar{t}$	7	7	7
Wt	3	3	3
Total background	10	10	10
S/B	4.1	21.5	1.6
S/\sqrt{B}	13.0	68.0	5.1

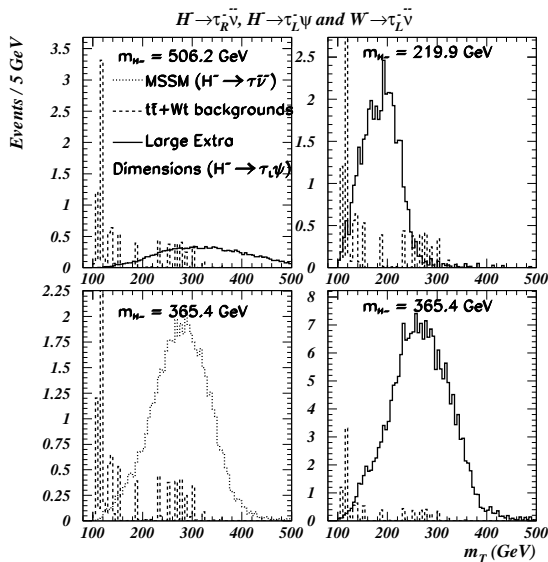


FIG. 12: The reconstructions of the transverse mass for the signal in MSSM, the signal in models with a singlet neutrino in large extra dimensions and for the backgrounds, for an integrated luminosity of 100 fb^{-1} . In general, an MSSM charged Higgs can be discovered at the LHC depending on m_A and $\tan\beta$. In the models with a singlet neutrino in large extra dimensions, the signal can also be discovered at the LHC depending on the parameters M_* , δ , m_D , m_A and $\tan\beta$. The observation of the signal in the transverse mass distribution would not be sufficient to identify the model: the τ polarization effects must be explored further.

IV. CONCLUSIONS

Large extra dimensions models with TeV scale quantum gravity assume the existence of additional dimensions where gravity – and possibly other fields – propagate. The size of the extra dimensions are constrained to the sub-millimeter level since no experimental deviations from the Newtonian gravity has been observed at distances larger than ~ 0.2 millimeter.

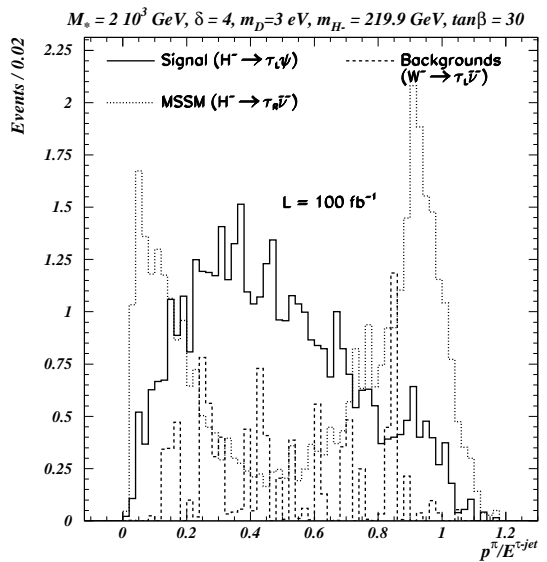


FIG. 13: The distribution of the ratio of the charged pion track momentum in one prong τ decay to the τ -jet energy for $m_A = 200 \text{ GeV}$, $\tan\beta = 30$, $M_* = 2 \text{ TeV}$, $\delta = 4$ and $m_\nu = 0.5 \cdot 10^{-3} \text{ eV}$. In the case shown here, the polarization asymmetry is ~ 1 ($\sim 100\%$ left handed τ^-). We see the difference between MSSM and large extra dimensions with singlet neutrino in the bulk. In Fig. 14, the difference between these two models is more pronounced due to the more significant signals.

In these models, the right handed neutrino can freely propagate into the extra dimensions because it has no quantum numbers to constrain it to the SM brane. The interactions between the bulk neutrino and the SM fields on the brane can generate Dirac neutrino masses consistent with the atmospheric neutrino oscillations without implementing the seesaw mechanism. There are no additional Higgs bosons required in these models. The charged Higgs productions are therefore the same as in the 2HDM.

The charged Higgs can decay to both the right and the

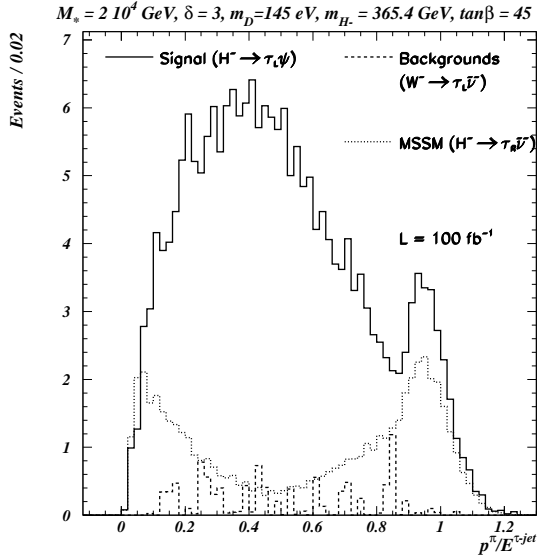


FIG. 14: The distribution of the ratio of the charged pion track momentum in one prong τ decay to the τ -jet energy for $m_A = 350$ GeV, $\tan \beta = 45$, $M_* = 20$ TeV, $\delta = 3$ and $m_\nu = 0.05$ eV. In the 2HDM-II, this ratio would peak near 0 and 1 as shown while in other models, the actual distribution of this ratio would depend on the polarization asymmetry since both left and right handed τ 's would contribute. In the case shown, the asymmetry is ~ 1 and the ratio peaks near the center of the distribution.

left handed τ -leptons, $H^- \rightarrow \tau_R^- \bar{\nu} + \tau_L^- \psi$ whereas in the 2HDM-II such as MSSM, only the right handed τ decay of the H^- is possible through the τ Yukawa coupling: $H^- \rightarrow \tau_R^- \bar{\nu}$. The τ decay of the charged Higgs has been studied in details for ATLAS and CMS. In the current study, we focus on the observability of $H^- \rightarrow \tau_L^- \psi$ at the LHC for Higgs masses larger than the top-quark mass.

The charged Higgs is generated through the $2 \rightarrow 2$ process, $gb \rightarrow tH^\pm$ — where $H^- \rightarrow \tau_R^- \bar{\nu} + \tau_L^- \psi$ — and we

require the hadronic decay of the associated top-quark: $t \rightarrow jjb$. The major backgrounds considered are the single top-quark production, $gb \rightarrow tW^\pm$ and the $t\bar{t}$ production with one $W^+ \rightarrow jj$ and the other $W^- \rightarrow \tau_L^- \bar{\nu}$. We include the τ polarization in the analysis and select one-prong hadronic τ decays since these events carry a better imprint of the τ polarization. Due to the neutrino in the final state, only the transverse mass can be reconstructed. In the backgrounds, the transverse mass has an upper bound at the W mass while in the signal, the bound is at the charged Higgs mass. As a result, above the W threshold, the background is relatively very small. Thus, the discovery reach of the charged Higgs in the $\tau\nu$ channel is limited by the signal size itself.

The mass of the neutrino ψ would be different on event by event basis. Consequently, the efficiencies of the kinematic cuts would somewhat be different. However, main results of the current analysis derive from the differences in the polarizations of the τ -lepton and in the transverse mass bounds, and would not be significantly affected by the neutrino mass effect.

Although the observation of a signal in the transverse mass distribution can be used to claim discovery of the charged Higgs, it is insufficient to pin down the scenario that is realized. Additionally, by reconstructing the fraction of the energy carried by the charged track in the one-prong τ decay, it is possible to claim whether the scenario is the ordinary 2HDM or not. The further measurement of the polarization asymmetry might provide a distinctive evidence for models with singlet neutrino in large extra dimensions.

Acknowledgments

K. A. Assamagan expresses gratitude to K. Agashe for fruitful discussions. This work was partially performed at the Les Houches Workshop: “Physics at TeV Colliders” 21 May – 1 June 2001. We thank the organizers for the invitation.

[1] T. Kaluza, Sitzungsber. Preuss. Akad. Wiss. Berlin (Math. Phys.) **K1**, 966 (1921); for a translation of the original paper see T. Muta, HUPD-8401 *in O’Raifeartaigh, L.: The dawning of gauge theory** 53-58; O. Klein, Z. Phys. **37**, 895 (1926) [Surveys High Energ. Phys. **5**, 241 (1926)].

[2] N. Arkani-Hamed, S. Dimopoulos and G. R. Dvali, Phys. Lett. B **429**, 263 (1998) [arXiv:hep-ph/9803315]; Phys. Rev. D **59**, 086004 (1999) [arXiv:hep-ph/9807344]; I. Antoniadis, N. Arkani-Hamed, S. Dimopoulos and G. R. Dvali, Phys. Lett. B **436**, 257 (1998) [arXiv:hep-ph/9804398]; G. F. Giudice, R. Rattazzi and J. D. Wells, Nucl. Phys. B **544**, 3 (1999) [arXiv:hep-ph/9811291]; E. A. Mirabelli, M. Perelstein and M. E. Peskin, Phys. Rev. Lett. **82**, 2236 (1999) [arXiv:hep-ph/9811337];

T. Han, J. D. Lykken and R. J. Zhang, Phys. Rev. D **59**, 105006 (1999) [arXiv:hep-ph/9811350].

[3] N. Arkani-Hamed, S. Dimopoulos, G. R. Dvali and J. March-Russell, arXiv:hep-ph/9811448. K. R. Dienes, E. Dudas and T. Gherghetta, Nucl. Phys. B **557**, 25 (1999) [arXiv:hep-ph/9811428].

[4] K. Akama, Lect. Notes Phys. **176**, 267 (1982) [arXiv:hep-th/0001113]; V. A. Rubakov and M. E. Shaposhnikov, Phys. Lett. B **125** (1983) 136; for a review see V. A. Rubakov, “Large and infinite extra dimensions: An Introduction,” arXiv:hep-ph/0104152.

[5] J. Polchinski, arXiv:hep-th/9611050. C. P. Bachas, arXiv:hep-th/9806199.

[6] C. D. Hoyle, U. Schmidt, B. R. Heckel, E. G. Adelberger, J. H. Gundlach, D. J. Kapner and H. E. Swanson, Phys.

Rev. Lett. **86**, 1418 (2001) [arXiv:hep-ph/0011014].

[7] S. P. Martin and J. D. Wells, Phys. Rev. D **60**, 035006 (1999) [arXiv:hep-ph/9903259].

[8] Y. Fukuda *et al.* [SuperKamiokande Collaboration], Phys. Rev. Lett. **82**, 2644 (1999) [arXiv:hep-ex/9812014]; **85**, 3999 (2000) [arXiv:hep-ex/0009001]; **86**, 5656 (2001) [arXiv:hep-ex/0103033]; A. Ioannisian and A. Pilaftsis, Phys. Rev. D **62**, 066001 (2000) [arXiv:hep-ph/9907522]. R. N. Mohapatra and A. Perez-Lorenzana, Nucl. Phys. B **576**, 466 (2000) [arXiv:hep-ph/9910474]; A. S. Dighe and A. S. Joshipura, Phys. Rev. D **64**, 073012 (2001) [arXiv:hep-ph/0105288]; A. De Gouvea, G. F. Giudice, A. Strumia and K. Tobe, arXiv:hep-ph/0107156.

[9] K.A. Assamagan and Y. Coadou, ATLAS Internal Note, ATL-PHYS-2000-031 (2000); K. A. Assamagan, Acta Phys. Polon. B **31**, 863 (2000).

[10] R. Kinnunen, “The $H^\pm \rightarrow \tau\nu$ mode in CMS” and “Signatures of Heavy Charged Higgs Bosons at the LHC”, in Les Houches Workshop (1999), “The Higgs working group: Summary report,” arXiv:hep-ph/0002258.

[11] R. Barbieri, P. Creminelli and A. Strumia, Nucl. Phys. B **585**, 28 (2000) [arXiv:hep-ph/0002199].

[12] T. Sjöstrand, “High-Energy Physics Event Generation with PYTHIA 5.7 and JETSET 7.4”, Comput. Phys. Commun. **82**, 74 (1994).

[13] E. Richter-Wąs, D. Froidevaux and L. Poggiali, ATLAS Internal Note, ATL-PHYS-98-131, (1998).

[14] S. Heinemeyer, W. Hollik and G. Weiglein, arXiv:hep-ph/0002213.

[15] A. Djouadi, J. Kalinowski and M. Spira, Comput. Phys. Commun. **108**, 56 (1998) [arXiv:hep-ph/9704448].

[16] K. Agashe, N. G. Deshpande and G. H. Wu, Phys. Lett. B **489**, 367 (2000) [arXiv:hep-ph/0006122].

[17] S. Jadach, Z. Wąs, R. Decker and J. H. Kühn, Comput. Phys. Commun. **76**, 361 (1993); M. Jezabek, Z. Wąs, S. Jadach and J. H. Kühn, Comput. Phys. Commun. **70**, 69 (1992); S. Jadach, J. H. Kühn and Z. Wąs, Comput. Phys. Commun. **64**, 275 (1990).

[18] S. Raychaudhuri and D. P. Roy, Phys. Rev. D **52**, 1556 (1995) [arXiv:hep-ph/9503251].